1997 IEEE Nuclear Science Symposium and Medical Imaging Conference Record, pages 1340–1344 (preprint)

Kinetic Parameter Estimation from Attenuated SPECT Projection Measurements[1]

BW Reutter[†], *Member, IEEE*; GT Gullberg[‡], *Senior Member, IEEE*;
and RH Huesman[†], *Senior Member, IEEE*
[†] Center for Functional Imaging, Lawrence Berkeley National Laboratory
University of California, Berkeley, CA 94720, USA
[‡] Department of Radiology, University of Utah, Salt Lake City, UT 84132, USA

Abstract

Kinetic parameters are commonly estimated from dynamically acquired nuclear medicine data by first reconstructing a temporal sequence of images and subsequently fitting the parameters to time-activity curves generated from regions of interest overlaid upon the image sequence. Biased estimates can result from images reconstructed using inconsistent projections of a time-varying distribution of radiopharmaceutical acquired by a rotating SPECT system. To overcome this problem we investigated the estimation of kinetic parameters directly from projection data by modeling the data acquisition process. To accomplish this it was necessary to parametrize the spatial and temporal distribution of the radiopharmaceutical within the SPECT field of view.

In a simulated transverse slice, kinetic parameters were estimated for simple one compartment models for three myocardial regions of interest, as well as for the liver. Myocardial uptake and washout parameters estimated by conventional analysis of noiseless simulated data had biases ranging between 1–63%. Parameters estimated directly from the noiseless projection data were unbiased as expected, since the model used for fitting was faithful to the simulation. Parameter uncertainties for 500,000 detected events ranged between 1–25% for the myocardial uptake parameters and 1–18% for the myocardial washout parameters.

I. Introduction

Kinetic parameters are commonly estimated from dynamically acquired nuclear medicine data by first reconstructing a temporal sequence of images and subsequently fitting the parameters to time-activity curves generated from regions of interest (ROIs) overlaid upon the image sequence. Since dynamic single photon emission computed tomography (SPECT) data acquisition involves movement of the gantry and the distribution of radiopharmaceutical changes during the acquisition, projections at different angles come from different tracer distributions. Images reconstructed from these inconsistent projections can contain artifacts that lead to biases in the estimated kinetic parameters. The artifacts can be particularly problematic in images reconstructed from projections acquired during the early time frames of a dynamic study when the tracer distribution is changing most rapidly (Fig. 1).

To overcome this problem we investigated the estimation of kinetic parameters directly from projection data by modeling the data acquisition process of a time-varying distribution of radiopharmaceutical detected by a rotating SPECT system. To accomplish this it was necessary to parametrize the spatial and temporal distribution of the radiopharmaceutical within the SPECT field of view.

Direct estimation of kinetic parameters from projections has become an active area of research. Chiao et al. [1, 2] have jointly estimated myocardial ROI boundaries and one-compartment kinetic model parameters directly from simulated positron emission tomography (PET) projections. Limber et al. [3] have fit single decaying exponentials to each pixel in a 16×16 array directly from simulated SPECT projections. We have fit one-compartment models to ROIs encompassing a 3×3 array directly from simulated SPECT projections, by first estimating the exponential factors using linear time-invariant system theory and then estimating the multiplicative coefficients using linear estimation [4].

Estimation of ROI time-activity curves from projections has been investigated. Huesman [5] has described a method to estimate the average activity in a 2-D ROI, and Defrise et al. [6] have extended these ideas to 3-D. To compensate for physical factors such as attenuation and detector resolution, Carson [7] has described a method for estimating activity densities assumed to be uniform in a set of ROIs using maximum likelihood, and Formiconi [8] has similarly used least squares.

The work presented here builds on the work of Carson and Formiconi, as well as on simulations which we have performed in 2-D and 3-D using idealized non-attenuating phantoms [4, 9, 10]. In this 2-D simulation we use the more realistic mathematical cardiac torso (MCAT) phantom [11] and include the effects of attenuation. We compare the estimation of kinetic parameters directly from projections with estimation from tomographic determination of time-activity curves, for three myocardial ROIs and for the liver.

II. Estimation of Kinetic Parameters Directly from Projections

We formulate a nonlinear estimation problem using a spatial and temporal parametrization of the time-varying distribution measured with a single rotating detector SPECT system. The one-compartment model shown in Fig. 2 is

[1]This work was supported by U.S. Department of Health and Human Services grant R01-HL50663 and by U.S. Department of Energy contract DE-AC03-76SF00098.

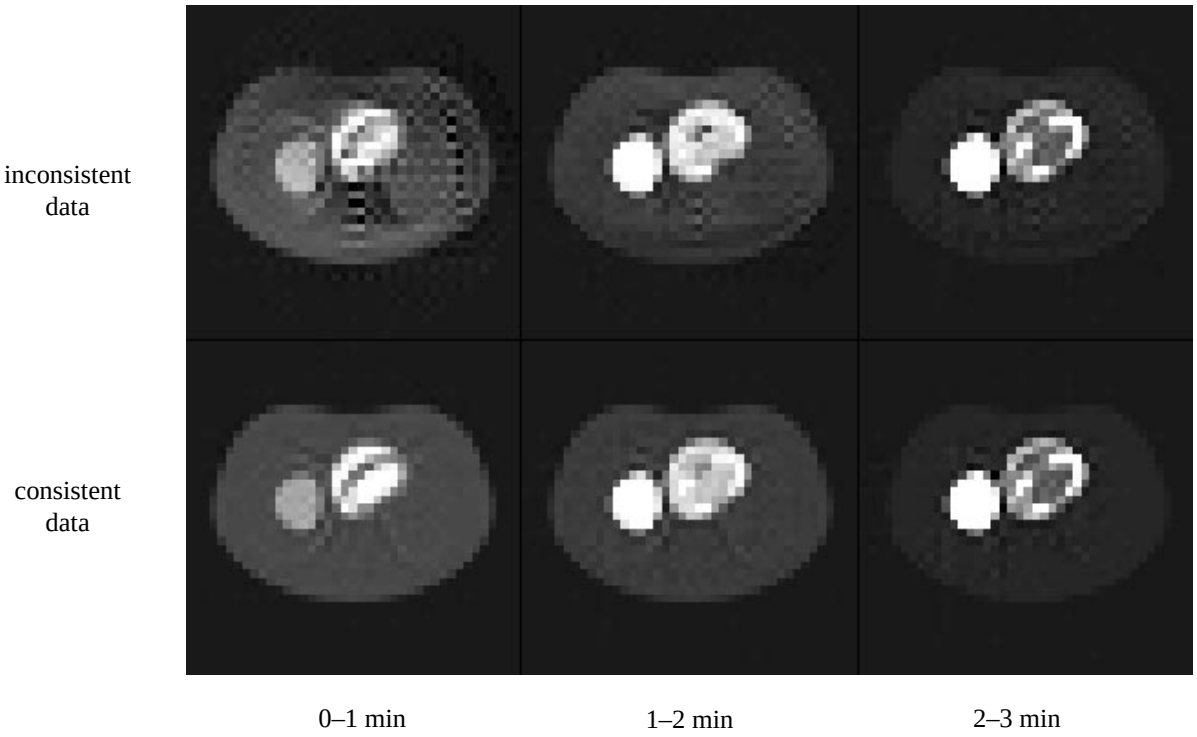

Fig. 1 Artifacts are apparent in the upper sequence of images reconstructed from the inconsistent projections of a relatively rapidly changing tracer distribution acquired during the early time frames of a simulated dynamic SPECT study. The lower sequence of images is obtained when the tracer distribution does not change during the time frames.

assumed for simulated myocardial and liver tissue with a known blood input function, which would correspond to the kinetics of teboroxime [12, 13, 14]. Parameters are estimated by minimizing a weighted sum of squared differences between the projections and the model predicted values.

The expression for uptake in tissue type m is

$$Q^m(t) = k_{21}^m \int_0^t B(\tau) e^{-k_{12}^m (t-\tau)} d\tau = k_{21}^m V^m(t), \quad (1)$$

where $B(t)$ is the known blood input function, k_{21}^m is the uptake parameter, and k_{12}^m is the washout parameter. Total activity in the tissue is given by

$$Q^m(t) + f_v^m B(t) = k_{21}^m V^m(t) + f_v^m B(t), \quad (2)$$

where f_v^m is the fraction of vasculature in the tissue.

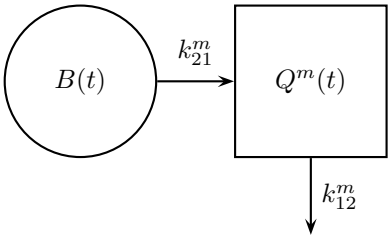

Fig. 2 Compartmental model for ^{99m}Tc-teboroxime in the myocardium.

This analysis starts with an image segmented into blood pool, M tissue types of interest, and background. In order to obtain tissue boundaries, the patient is assumed motionless during data acquisition, and a reconstructed image (for example, via the projections at the time of strongest signal, or via the summed projections) is segmented to provide anatomical structure. The image intensity at each segmented region is not used.

Using the segmented image and a measured attenuation distribution, the attenuated static projections of the blood pool, tissue, and background regions are calculated for each projection ray of each projection angle. These are the sinograms that would be observed for each region, given a static unit concentration of activity within the region. With no attenuation, the static projections correspond to the lengths of the blood pool, tissue, and background regions along each projection ray of each projection angle.

The number of projection rays per projection angle is denoted by N, the number of projection angles per rotation by J, and the number of rotations by I. Thus, there are a total of IJN projection rays distributed in time and space. For a typical projection ray at angle j and position n, the attenuated static projections of the blood pool, background, and tissue m are denoted by u_{jn}, v_{jn}, and w_{jn}^m, respectively. Fig. 3 shows the attenuated static projections of the ROIs in the MCAT phantom (Figs. 4 and 5) used in the computer simulations described in Section III. The amplitude of the background activity is denoted by g, and the background is assumed to be

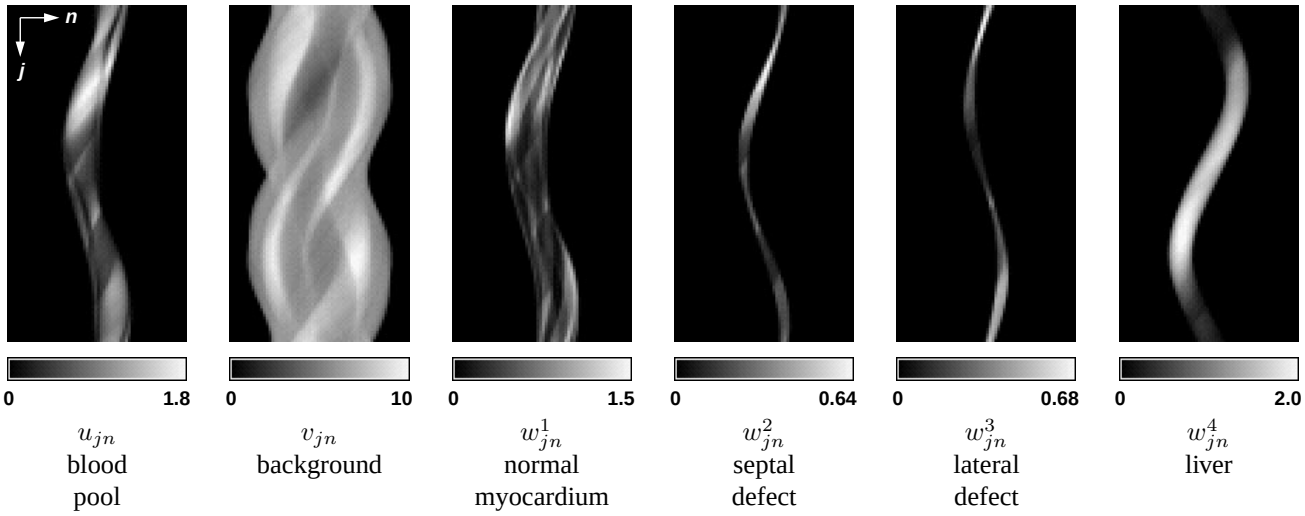

Fig. 3 Attenuated static projections of the ROIs in the MCAT phantom shown in Figs. 4 and 5. These are the sinograms that would be observed for each region, given a static unit concentration of activity within the region.

proportional to the blood activity. The projection equations can be expressed as

$$p_{ijn} = \int_{t_{ij}-\Delta t}^{t_{ij}} \left\{ u_{jn} B(\tau) + v_{jn} g B(\tau) + \sum_{m=1}^{M} w_{jn}^m \left[k_{21}^m V^m(\tau) + f_v^m B(\tau) \right] \right\} d\tau \ , \quad (3)$$

where the time t_{ij} is equal to $[j + (i-1)J]\Delta t$. The constants u_{jn}, v_{jn}, and w_{jn}^m are pure geometrical weighting factors, and the projection equations are linear in the unknowns g, k_{21}^m, and f_v^m. The nonlinear parameters, k_{12}^m, are contained in $V^m(t)$.

The criterion which is minimized by varying the model parameters is the weighted sum of squares function

$$\chi^2 = \sum_{i=1}^{I} \sum_{j=1}^{J} \sum_{n=1}^{N} \frac{(p_{ijn} - p_{ijn}^*)^2}{\sigma_{ijn}^2} \ , \quad (4)$$

where p_{ijn}^* are the measured data and σ_{ijn} are their statistical uncertainties. An estimate of the covariance matrix for the resulting model parameters $\hat{\Theta} = (\ \hat{k}_{12}^m \quad \hat{g} \quad \hat{k}_{21}^m \quad \hat{f}_v^m\ )$ is

$$\mathrm{cov}(\hat{\Theta}) = \left(\frac{1}{2} \frac{\partial^2 \chi^2}{\partial \Theta^2} \bigg|_{\Theta=\hat{\Theta}} \right)^{-1} . \quad (5)$$

The statistical uncertainties of the parameter estimates, $\hat{\Theta}$, are the square roots of the diagonal elements of the covariance matrix given by (5).

As discussed above, (3) is a linear function of the parameters g, k_{21}^m, and f_v^m. Therefore the model it describes is called a conditionally linear, partially linear, or separable nonlinear model [15, 16]. Using standard techniques for removing conditionally linear parameters, (4) can be considered to be a function of only the nonlinear washout parameters, k_{12}^m. We have used this technique to obtain the results presented here.

III. Computer Simulations

A transverse slice of the MCAT phantom was used in a simulation to evaluate the ability to estimate kinetic parameters directly from attenuated SPECT projection data. The simulated emission distribution, shown in Fig. 4, contained blood, background, liver, and three myocardial regions of interest (normal myocardium, septal defect, and lateral defect). The emission distribution was assumed to be attenuated using the attenuation distribution shown in Fig. 5, calculated for 140 keV. The blood input function and the simulated tissue activity curves are shown in Fig. 6.

There were 13 parameters to estimate: the amplitudes, decay rates, and vascular fractions for the liver and the three myocardial regions and the amplitude of the overall background. Using these 13 parameters and the known blood input function, a dynamic sinogram was formed representing the attenuated projections of the six constituent components (blood, background, liver, normal myocardium, septal defect, lateral defect), which comprise the image volume. The 15 min data acquisition protocol consisted of 15 revolutions of a single-head SPECT system, acquiring 120 angles per revolution and 64 parallel projection samples per angle. Neither scatter nor geometric point response were included in the simulation.

Parameters were estimated by minimizing a weighted sum of squared differences between the projection data and the model predicted values (4). The results of the simulation are shown in Table 1 and Fig. 7. Direct parameter estimation from noiseless inconsistent projections (column d of Table 1) was compared with estimation from dynamic reconstructions (column b). Fifteen 41×41 attenuation corrected reconstructions were formed by using 30 iterations of the conjugate gradient algorithm [17]. Thirty iterations were sufficient to assure that the reconstructions had converged. Line-length weighting was used in the formulation of the projections. The pixel width was 1.5 times the bin width.

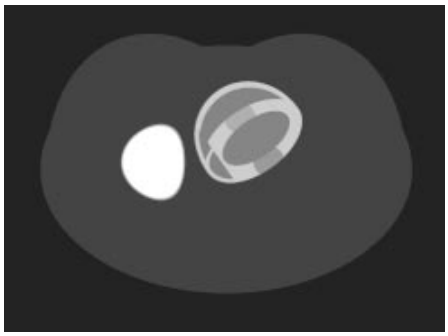

Fig. 4 MCAT emission phantom used in simulation.

Fig. 5 MCAT attenuation phantom used in simulation.

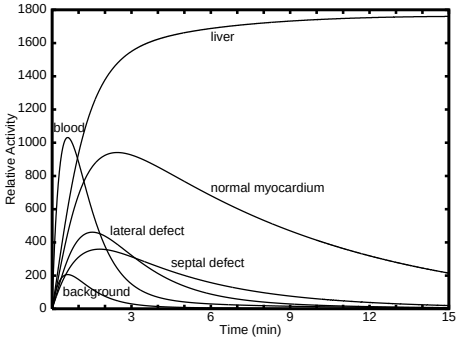

Fig. 6 Simulated time-activity curves for regions-of-interest.

ROIs were defined by taking all homogeneous blood pool, background, and liver pixels, as well as all pixels containing at least 90% of one of the three myocardial tissue types. Direct parameter estimation from projections was also compared to the direct estimation of region time-activity curves (column c) using the method proposed by Formiconi [8].

Parameter estimates obtained from conventional analysis of noiseless inconsistent projections had biases ranging between 5–63% for the myocardial uptake parameters and 1–61% for the myocardial washout parameters. The large biases in the septal and lateral defects are not unexpected considering the long tomographic acquisition times of 1 min. The estimates using Formiconi's method had less bias in the septal defect and more bias in the normal myocardium and the lateral defect, compared to the conventional method. Parameters estimated directly from the noiseless projection data were unbiased as expected, since the model used for fitting was faithful to the simulation. In addition, multiple local minima were not encountered regardless of noise levels simulated. Parameter uncertainties for 500,000 detected events (column e) ranged between 1–25% for the myocardial uptake parameters and 1–18% for the myocardial washout parameters.

Parameter estimates were also obtained from noiseless projections forced to be consistent over the 1 min time frame of the simulated dynamic data acquisition. Over the course of each revolution of the SPECT system, the activity in each region was held constant at the average of the continuously varying value that yielded the inconsistent projections. For the conventional analysis the biases changed very little for the main myocardium and were reduced substantially for the septal and lateral defects (column b′). The estimates obtained using Formiconi's method were unbiased for the forced consistent projections, as expected (column c′).

IV. Summary

The combination of gantry motion and the time-variation of the radiopharmaceutical distribution being imaged results in inconsistent projection data sets. Estimating kinetic parameters from time-activity curves taken from reconstructed images results in biases. Some of these biases are reduced and some are increased if the time-activity curves are estimated from the projection data [8]. Estimating the kinetic parameters directly from the projections removes all bias for faithfully modeled noiseless data. Implementation of this strategy requires a spatial and temporal model of the distribution of radiopharmaceutical with the SPECT field of view.

V. References

[1] P C Chiao, W L Rogers, N H Clinthorne, J A Fessler, and A O Hero. Model-based estimation for dynamic cardiac studies using ECT. *IEEE Trans Med Imag*, 13(2):217–226, 1994.

[2] P C Chiao, W L Rogers, J A Fessler, N H Clinthorne, and A O Hero. Model-based estimation with boundary side information or boundary regularization. *IEEE Trans Med Imag*, 13(2):227–234, 1994.

[3] M A Limber, M N Limber, A Celler, J S Barney, and J M Borwein. Direct reconstruction of functional parameters for dynamic SPECT. *IEEE Trans Nucl Sci*, 42(4):1249–1256, 1995.

[4] G L Zeng, G T Gullberg, and R H Huesman. Using linear time-invariant system theory to estimate kinetic parameters directly from projection measurements. *IEEE Trans Nucl Sci*, 42(6):2339–2346, 1995.

[5] R H Huesman. A new fast algorithm for the evaluation of regions of interest and statistical uncertainty in computed tomography. *Phys Med Biol*, 29(5):543–552, 1984.

[6] M Defrise, D Townsend, and A Geissbuhler. Implementation of three-dimensional image reconstruction for multi-ring positron tomographs. *Phys Med Biol*, 35(10):1361–1372, 1990.

[7] R E Carson. A maximum likelihood method for region-of-interest evaluation in emission tomography. *J Comput Assist Tomogr*, 10(4):654–663, 1986.

[8] A R Formiconi. Least squares algorithm for region-of-interest evaluation in emission tomography. *IEEE Trans Med Imag*, 12(1):90–100, 1993.

[9] R H Huesman, B W Reutter, G L Zeng, and G T Gullberg. Kinetic parameter estimation from SPECT projection measurements. *J Nucl Med*, 38(5 suppl):222P–223P, 1997. (abstract).

[10] R H Huesman, B W Reutter, G L Zeng, and G T Gullberg. Kinetic parameter estimation from SPECT cone-beam projection measurements. In P Kinahan and D Townsend, editors, *1997 International Meeting on Fully 3-D Image Reconstruction and Nuclear Medicine Conference Record*, pages 121–125, 1997. (abstract).

[11] J A Terry, B M W Tsui, J R Perry, and G T Gullberg. A three-dimensional mathematical phantom of the human torso for use in

		a	b	c	d	e	b′	c′
normal myocardium	k_{21}^1	0.700	0.665	0.767	0.700	0.009	0.669	0.700
	k_{12}^1	0.150	0.149	0.162	0.150	0.002	0.152	0.150
	f_v^1	0.150	0.160	-0.032	0.150	0.022	0.187	0.150
septal defect	k_{21}^2	0.300	0.112	0.314	0.300	0.060	0.291	0.300
	k_{12}^2	0.300	0.116	0.286	0.300	0.048	0.279	0.300
	f_v^2	0.100	0.394	0.110	0.100	0.097	0.134	0.100
lateral defect	k_{21}^3	0.500	0.218	0.096	0.500	0.126	0.480	0.500
	k_{12}^3	0.600	0.247	0.214	0.600	0.105	0.467	0.600
	f_v^3	0.100	0.278	0.199	0.100	0.115	0.137	0.100
liver	k_{21}^4	0.900	0.924	0.888	0.900	0.005	0.923	0.900
	k_{12}^4	0.0020	0.0020	0.0006	0.0020	0.0006	0.0020	0.0020
	f_v^4	0.200	0.236	0.325	0.200	0.012	0.198	0.200
background	g	0.200	0.200	0.201	0.200	0.001	0.199	0.200

Table 1

Results of kinetic parameter estimation from noiseless inconsistent projections: (a) simulated values; (b) values from dynamic reconstructions; (c) values from direct estimation of region time-activity curves [8]; (d) values from direct estimation from projections; (e) estimated uncertainties of values from direct estimation for 500,000 detected events using (5). Results of kinetic parameter estimation from noiseless consistent projections: (b′) values from dynamic reconstructions; (c′) values from direct estimation of region time-activity curves [8]. Units for uptake k_{21}^m and washout k_{12}^m are min^{-1}.

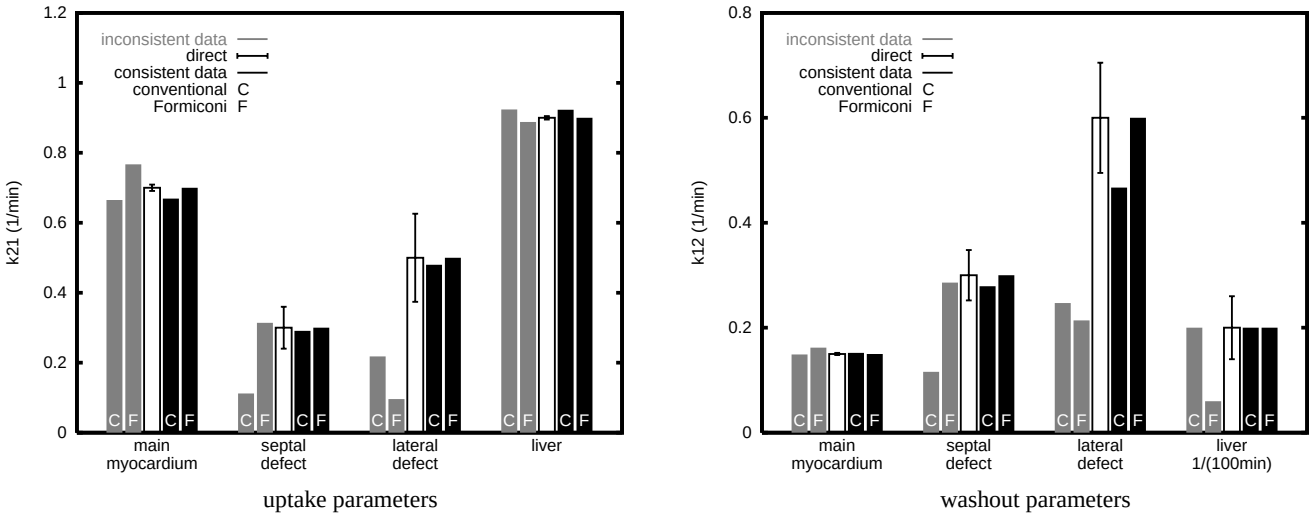

Fig. 7 Estimated values for the uptake parameters k_{21}^m (left) and the washout parameters k_{12}^m (right). The gray bars depict the estimates obtained from conventional and Formiconi analyses of noiseless inconsistent projections (columns b and c in Table 1). The white bar depicts the unbiased estimate (i.e., the simulated value) obtained directly from the projections, along with its estimated uncertainty predicted for 500,000 events using (5). The black bars depict the estimates obtained from conventional and Formiconi analyses of noiseless consistent projections (columns b′ and c′). Note that the units for the liver washout parameter, k_{12}^4, are (100 min)$^{-1}$.

SPECT imaging research studies. *J Nucl Med*, 31(5 suppl):868, 1990. (abstract).

[12] R K Narra, T Feld, and A D Nunn. Absorbed radiation dose to humans from technetium-99m-teboroxime. *J Nucl Med*, 33(1):88–93, 1992.

[13] A M Smith, G T Gullberg, P E Christian, and F L Datz. Kinetic modeling of teboroxime using dynamic SPECT imaging of a canine model. *J Nucl Med*, 35(3):984–995, 1994.

[14] A M Smith, G T Gullberg, and P E Christian. Experimental verification of ^{99m}Tc-teboroxime kinetic parameters in the myocardium using dynamic SPECT: Reproducibility, correlations to flow, and susceptibility to extravascular contamination. *J Nucl Cardiol*, 3:130–142, 1996.

[15] D M Bates and D G Watts. *Nonlinear Regression Analysis and Its Applications*. John Wiley & Sons, New York, 1988.

[16] G A F Seber and C J Wild. *Nonlinear Regression*. John Wiley & Sons, New York, 1989.

[17] R H Huesman, G T Gullberg, W L Greenberg, and T F Budinger. Donner algorithms for reconstruction tomography. Publication PUB-214, Lawrence Berkeley Laboratory, 1977.

1997 IEEE Nuclear Science Symposium and Medical Imaging Conference Record, pages 1340–1344 (preprint)